10-1-2010

Biocompatibility of Synthetic Poly(Ester urethane)/Polyhedral Oligomeric Silsesquioxane Matrices with Embryonic Stem Cell Proliferation and Differentiation

Yan-Lin Guo
University of Southern Mississippi, Yanlin.Guo@usm.edu

Wenshou Wang

Joshua U. Otaigbe
University of Southern Mississippi

Published in final edited form as:
J Tissue Eng Regen Med. 2010 October ; 4(7): 553–564. doi:10.1002/term.272.

Biocompatibility of Synthetic Poly(ester urethane)/Polyhedral Oligomeric Silsesquioxane Matrices with Embryonic Stem Cell Proliferation and Differentiation

Yan-Lin Guo[1,*], **Wenshou Wang**[2], and **Joshua U. Otaigbe**[2]

[1] Department of Biological Sciences, The University of Southern Mississippi, Hattiesburg, MS 39406

[2] School of Polymers & High Performance Materials, The University of Southern Mississippi, Hattiesburg, MS 39406

Abstract

Incorporation of polyhedral oligomeric silsesquioxanes (POSS) into poly (ester urethane)s (PEU) as a building block results in a PEU/POSS hybrid polymer with increased mechanical strength and thermostability. An attractive feature of the new polymer is that it forms a porous matrix when cast in the form of a thin film, making it potentially useful in tissue engineering. In this study, we present detailed microscopic analysis of the PEU/POSS matrix and demonstrate its biocompatibility with cell culture. The PEU/POSS polymer forms a continuous porous matrix with open pores and interconnected grooves. From SEM image analysis, it is calculated that there are about 950 pores per mm^2 of the matrix area with pore size ranging from 1 to 15 μm in diameter. The area occupied by the pores represents approximately 7.6 % of matrix area. Using mouse embryonic stem cells (ESCs), we demonstrate that the PEU/POSS matrix provides excellent support for cell proliferation and differentiation. Under the cell culture condition optimized to maintain self-renewal, ESCs grown on a PEU/POSS matrix exhibit undifferentiated morphology, express pluripotency markers, and have similar growth rate to cells grown on gelatin. When induced for differentiation, ESCs underwent dramatic morphological change, characterized by the loss of clonogenecity and increased cell size with well-expanded cytoskeleton networks. Differentiated cells are able to form a continuous monolayer that is closely embedded on the matrix. The excellent compatibility between the PEU/POSS matrix and ESC proliferation/differentiation demonstrates the potential of using PEU/POSS polymers in future ESC-based tissue engineering.

Keywords

Embryonic stem cell; Self-renewal; Differentiation; Poly (ester urethane)s; Polyhedral oligomeric silsesquioxanes; Cell-matrix interaction

1. Introduction

The goal of tissue engineering is to restore the function and structure of the damaged or aging tissues through the delivery of cells in appropriate matrices into the patient. Therefore, obtaining sufficient amount of cells and suitable matrices for cell growth are the two most

[*]Yan-Lin Guo, Ph.D. (To whom all correspondence should be addressed), Department of Biological Sciences, The University of Southern Mississippi, 118 College Drive # 5018, Hattiesburg, MS 39406, Tel; (601) 266-6018; Fax: (601) 2 66-5797, yanlin.guo@usm.edu.

important tasks in tissue engineering (Langer and Vacanti 1993). The natural biopolymers have been extensively explored for this purpose. However, most of them do not have proper mechanical properties. Their limited availability, immune rejection, and chemical complexity significantly limit their applications in tissue engineering (Burdick and Vunjak-Novakovic 2000; Saha et al. 2007). Consequently, there is an increasing need to develop synthetic materials as alternatives. Exciting advance in the field has been made in recent years driven by the rapid progress in stem cell biology and our ability to manufacture novel biomaterials in chemical engineering (Elisseeff et al. 2006). It is apparent that continued progress in this field will depend upon availability and reproducible technologies for manufacturing synthetic growth matrices.

The choice of the cells for tissue engineering is of critical importance. The limited availability of cells in sufficient quantity is one of the major barriers. Recent attention has been focused upon the use of stem cells, including adult stem cells and embryonic stem cells (ESCs), but the latter have been the center of intensive investigation (Wobus and Boheler 2005). It has become increasingly clear that ESCs could be a promising cell source for tissue engineering because of their availability in large quantity and the ability to differentiate to any types of somatic cells (Chai and Leong 2007; Dawson et al. 2008). ESCs are derived from the inner cell mass of an early stage embryo. Under proper culture conditions, they have unlimited capacity for self-renewal to produce large amount of cell stock. When induced, they can differentiate into desired cell lineages, a property known as pluripotency (Wobus and Boheler 2005). However, the lack of appropriate growth matrices and methods that maintain the pluripotency and directed differentiation of ESCs on demand to particular cell lineages is a major obstacle for their biomedical application (Raghunath et al. 2005; Wang et al. 2006). It is well recognized that both self-renewal and differentiation of ESCs are regulated by soluble growth factors, cytokines, other small molecules, and by the extracellular matrix(ECM). The ECM plays multiple roles for tissue function, but its primary function is to provide structural support to the cells and environmental cues that regulate cell activities (Nelson and Bissell 2006). Therefore, seeking synthetic matrices that mimic the mechanical properties and the surface chemistry of the natural ECM suitable for ESC propagation and controlled differentiation is one of the current focuses in ESC-based tissue engineering. Driven by the rapid advance in ESC research in recent years, various synthetic materials, such as polyamide-based 3D nanofibrillar (Nur et al. 2006), poly (ethylene terephthalate) matrix (Ouyang et al. 2007) and hydrogels (Gerecht et al. 2007) have been tested. Studies have shown the great promise of using these synthetic matrices for ESC expansion and differentiation (Gerecht et al. 2007; Hwang et al. 2006; Saha et al. 2007). Apparently, specific investigation will be needed for each of the polymeric matrices of interest because of their diverse chemical compositions and mechanical properties that can differentially affect ESC activities.

Polyurethane (PU) polymers are multiple micro-phase separated co-polymers consisting of soft and hard segments. This characteristic gives the polymers greater elasticity due to the flexible soft segments while the hard segments contribute to the mechanical strength (Korley et al. 2006; Wang et al. 2008). PU polymers can be tailored to various properties by varying the preparation methods and chemical compositions. A number of PU polymers have been used for biomedical devices, especially in the area of cardiovascular engineering (Kannan et al. 2005; Lamba et al. 1997). We have recently synthesized and characterized a novel biodegradable and biocompatible poly (ester-urethane)s (PEU). The PEU thin films support proliferation of several types of cells including ESCs without any toxicity (Wang et al. 2008). We are inspired by the recent finding that polyhedral oligomeric silsesquioxane (POSS), an organosilicon oligomer existing as a nanoscale hollow cage, can be incorporated into PU polymers as a building block (Kannan et al. 2005). It has been shown that incorporation of POSS into poly (carbonate-urea)urethane resulted in a hybrid polymer with

improved mechanical properties that also inhibits thromobogenicity (Kannan et al. 2006a) and promote endothelialization (Kannan et al. 2006b; Kannan et al. 2006c). These properties make this new class of polymers very attractive biomaterials for cardiovascular tissue engineering. We have developed alternative approaches of incorporating POSS molecules as an integral part of PEU chain segments (Nanda et al. 2006; Wang et al. 2009). An important finding is that the PEU/POSS hybrid polymer forms a porous matrix with when cast in the form of a thin film, a desired feature of cell growth matrices since porosity is critical for the nutrient/waste exchange in engineered tissues (Burdick and Vunjak-Novakovic 2000; Dawson et al. 2008; Hwang et al. 2008). In the current study, we describe the characterization of the porous PEU/POSS matrix and demonstrate its excellent compatibility with ESC proliferation and differentiation, therefore, its potential application in ESC-based tissue engineering and regenerative medicine.

2. Materials and Methods

2.1. Synthesis of PEU/POSS polymer and the film matrix preparation

The PEU/POSS hybrid polymer was synthesized via *in situ* homogeneous solution polymerization as we previously described in detail (Wang et al. 2009). For the film preparation, PEU/POSS polymer containing 6 wt% POSS was dissolved in dimethylformamide (DMF) and was then precipitated in ethanol. The precipitated PEU/POSS polymer was dried under vacuum for 48 h at 40 °C. A solution of 2% PEU/POSS was made in DMF. 140 μL of polymer solution was carefully dropped onto a coverglass (12 mm diameter) to form a thin film. The coverglasses were left at room temperature for 48 h, and then were further dried under vacuum for additional 48 h. They were sterilized in 70% ethanol overnight and thoroughly washed with PBS before use for cell culture.

2.2. Cell culture

Mouse ESCs (DBA/252 cell line) used in this study have been previously described (Allen et al. 2000; Guo and Yang 2006). They were maintained in standard ESC medium (knockout-DMEM, 15% fetal bovine serum [FBS], 0.2 mM L-glutamine, 0.1 mM 2-mercaptoethanol, 0.1 mM MEM nonessential amino acids, and 1000 U/ml LIF). Cells were routinely grown in cell culture dishes coated with 0.1% gelatin at 37°C in a humidified atmosphere at 5% CO_2.

Gelatin is a partial hydrolytic product of collagens that has been routinely used as a matrix protein to coat cell culture dishes for in vitro ESC proliferation and differentiation. For comparative analysis, gelatin-coated coverglasses were used in parallel experiments with the PEU/POSS thin matrix. For ESC proliferation, cells were cultured in standard ESC medium containing LIF to prevent differentiation. After incubated for different time periods, the cells were fixed and stained with 1% toluidine blue (TB). The cells density was examined under a microscope. To quantitatively determine cell number, TB was extracted with 2% sodium dodecyl sulfate. The absorbance at 630 nm was determined with a microtiter plate reader. The value, which correlates with cell number, was used as an indirect measurement of cell proliferation as previously described (Wang et al. 2008). For differentiation, cells were cultured under the same conditions as described for cell proliferation except that the LIF was excluded to promote cell differentiation. The medium was refreshed every other day. After differentiation for 10 days, the cells were fixed with 4% paraformaldehyde and processed for various microscopic analyses as described in individual experiments.

2.3. Colony formation and alkaline phosphatase (AP) assay

ESCs were seeded onto coverglasses coated with gelatin or coated with the PEU/POSS matrix and cultured in standard ESC medium for 6 days under the same conditions as

described for cell proliferation. The medium was refreshed every day. At the end of the experiment, cells were fixed with 4% paraformaldehyde and stained with an AP Kit (Sigma)following the procedures recommended by the manufacturer. AP positive colonies, which indicate the undifferentiated state of ESCs (O'Connor et al. 2008), were identified by their red color and analyzed under a microscope.

2.4. Quantitative real time-PCR (qRT-PCR) analysis

The expression level of ESC pluripotency markers was analyzed by qRT-PCR according the method we previously described (Chakraborty et al. 2009). Briefly, total RNA was extracted from cells with Tri-reagent (Sigma) and treated with DNase to eliminate residual genomic DNA. cDNA was prepared by reverse transcription using M-MLV reverse transcriptase. The specificity of PCR products was determined by dissociation curve and confirmed by agarose gel electrophoresis. qRT-PCR was performed using the SYBR green jumpstart TAQ ready mix (Sigma) on a MX3000PTM Real-time PCR system (Stratagene). Sequences for the primer sets for ESC pluripotency markers were as follows:

Sox2, forward: 5′-GACAGCTACGCGCACATGA-3′

reverse: 5′-GGTGCATCGGTTGCATCTG-3′

Oct4, forward: 5′-AGTTGGCGTGGAGACTTTGC-3′

reverse:5′-CAGGGCTTTCATGTCCTGG-3′

Nanog, forward: 5′-TTGCTTACAAGGGTCTGCTACT-3′

reverse: 5′-ACTGGTAGAAGAATCAGGGCT-3′

β-actin, forward: 5′-CATGTACGTAGCCATCCAGGC-3′

reverse: 5′-CTCTTTGATGTCACGCACGAT-3′

The mRNA level from qRT-PCR was calculated using the comparative Ct method (Pfaffl 2001). β-actin mRNA was used as a calibrator for the calculation of relative mRNA levels of the tested genes.

2.5. Microscopy and image analysis

Phase contrast microscopy—Cells stained with AP staining kit or with TB were analyzed under an inverted Olympus microscope with phase contrast lenses and photographed with a Cannon digital camera.

Fluorescence and confocal microscopy—To visualize the cytoskeleton and the nuclei, the cells were double stained with uorescein isothiocyanate (FITC)-phalloidin (5 μg/ml) and DAPI (10 μM), respectively. The cells were examined under an Olympus fluorescence microscope (BX60). The images were photographed with a micropublisher digital camera (Qimaging). To visualize the auto-fluorescence of the polymer films, the samples were examined under a Nikon fluorescence microscope (Eclipse 80i) with filters set for the examination of FITC. The images were processed using Image-Pro Plus software. To visualize the surface structure and cell-matrix interaction, a Z-stack consisting of a series of sections with the thickness of 1.5 μm per section were acquired with LSM510 laser-scanning confocal microscope (Zeiss). The 3D projection was reconstructed from Z-stack sections with LSM Image Examiner software (Zeiss).

Scanning electron microscopy (SEM)—Cells grown on glass coverglasses coated with gelatin or with the PEU/POSS matrix were fixed with 4% paraformaldehyde. The cells were dehydrated with ethanol with increment from 35% of ethanol to 100%. The surfaces of

the samples were sputter-coated with gold at 25 mA for 150 seconds to increase the electrical conductivity and then analyzed with a SEM (FEI Quanta 200) under high vacuum at 20 kv. The images were captured at different magnifications. Quantitative analysis of the pore size, number, distribution, and area coverage in the PEU/POSS matrix were performed with an image analysis software (Image J®).

3. Results

3.1. Characterization of the porous PEU/POSS matrix

We have previously reported that incorporation of POSS into PEU influence a number of physical and mechanical properties, such as storage modulus, viscosity, surface property, and degradability (Nanda et al. 2006; Wang et al. 2009). While testing cell growth on PEU/POSS matrices, we unexpectedly found that the structural features of PEU/POSS thin films could be visualized under a fluorescence microscope due the auto-fluorescence of the polymers. Figure 1A shows the structure of a thin film visualized under a conventional fluorescence microscope. It appears as a continuous porous matrix with a regular pattern of pores and grooves. To confirm this observation, the thin film was subjected to further analysis by confocal microscopy and scanning electron microscopy (SEM). Figure 1B shows the 3D surface structure of the thin film reconstructed from a Z-stack of thin sections, reflecting the grooves observed by conventional fluorescence microscopy. Although these structures distribute randomly, the overall surface of the matrix appears rather uniform with average thickness of ~30 μm. The images from SEM share similar structural characteristics detected by fluorescence microscopy but reveal more details. The open pores are clearly visible (Figure 1C & D, indicated by arrows). They vary in diameter ranging approximately from 1 to 15 μm and randomly distributed through out entire imaged area. Using the Image J® software, the pores in SEM images were traced to new images where the pore number and area can be automatically calculated. Figure 1E and F show the results and data corresponding to Figure 1C and D, respectively. It is calculated that there are about 950 pores/per mm^2, which collectively cover about 7.6 ± 1.35% of total imaged area of the matrix (determined from 3 images). It is noted that number of pores from the automatic calculation with the software is very close the results obtained by manual counting and that the dimension and the distribution of pores generated in the new images closely match that observed in the original images (E vs. C and F vs. D).

3.2. The PEU/POSS matrix can support ESC proliferation and maintain ESC pluripotency

To test if the surface structure of the PEU/POSS thin film is compatible with ESC growth, we first analyzed ESC adhesion and proliferation on a PEU/POSS matrix. ESCs were seeded at the low density and cultured for 1, 2, and 3 days. The cells on the polymers were not visible due to the similar color between the polymer and live cells, but cells can be easily identified by their purple color after staining them with toluidine blue (TB). As shown in figure 2A, ESCs grew in colonies as expected on a gelatin-coated coverglass. ESCs grown on a PEU/POSS matrix were also detected as colonies with similar size and cell density to cells grown on gelatin. To quantitatively determine growth rate at different growth periods, TB was extracted from the stained cells. As shown in figure 2B, the number of cells grown on gelatin and PEU/POSS matrices is similar at all three time periods tested. It is noted that cells grown on a thin film matrix can be released from by trypsin and subcultured in a new cell culture dish or a polymer matrix.

To examine the cell and colony morphology, TB-stained cells were analyzed under a high magnification of a phase contract microscope. The cells and the colonies grown on gelatin can be clearly visualized, but sharply focused images of cells and colonies could not be obtained (Figure 3A). However, the details of cell and colony morphology were better

visualized with SEM. A distinctive feature revealed is that the colonies grown on gelatin are flattened with protrusions at the edge of the colonies while cells in the colonies on a PEU/POSS matrix are round with smooth surface (Figure 3B).

ESCs express alkaline phosphatase (AP), which has been widely used as a reliable marker of undifferentiated state of ESCs (O'Connor et al. 2008). We investigated whether the PEU/POSS matrix affected the pluripotency of ESCs grown on a PEU/POSS matrix. As shown in figure 4, compact colonies with different sizes grown on both gelatin and a PEU/POSS matrix were detected by AP staining with comparable intensity (red color, AP, upper panels). The AP stained samples were further stained with toluidine blue to show total number of cells (TB, lower panels). Judging from the ratio of AP positive colonies (middle panels) to the total colonies (lower panels), the number of AP positive colonies on gelatin and on the PEU/POSS matrix is comparable, indicating the cells grown on the two matrices are in similar undifferentiated state.

The AP staining is a sensitive but not a quantitative method for the assessment of ESC pluripotency. Therefore, we further analyzed the expression of ESC marker genes, Oct4, Sox2, and Nanog, three major genes that are responsible for the maintenance of ESC pluripotency and self-renewal (Niwa et al. 1998). We quantitatively determined the expression of Oct4, Sox2, and Nanog at the mRNA level by real-time RT-qPCR. As shown in figure 5, their expression levels were similar in ESCs grown on gelatin and the PEU/POSS matrix, which is in agreement with the result determined with AP staining, indicating that the PEU/POSS matrix does not affect ESC self-renewal capacity in comparison with gelatin under the conditions that are optimized for ESC self-renewal.

3.3. The PEU/POSS matrix supports ESC differentiation

Undifferentiated ESCs are characterized by small cell bodies with a large nucleus and growing in aggregates (Figure 6A, cells stained with TB). The small volume of cytoplasm can be indirectly viewed by the cytoskeleton as a small portion between adjacent cells when cells were stained with FITC-phalloidin for actin filaments (Figure 6B, green, the large oval empty spaces are occupied by nuclei). The combination of these two cell staining methods can be conveniently used to detect the morphological change during ESC differentiation. When cultured in the absence of LIF, ESCs undergo spontaneous differentiation in the presence of serum, characterized by the loss of colonogenecity and the change of morphology. Although differentiated cells under this condition represent a heterogeneous population of different types of cells, most cells are significantly larger than undifferentiated cells and have flattened cell morphology. Cells with similar morphology often exist in a group. Figure 6C, D, & E show a group of differentiated cells on gelatin and analyzed by phase contrast microscopy (C, TB stained cells), fluorescence microscopy (D, FITC-phalloidin-labeled cells), and SEM (E). The large flattened individual cells can be clearly distinguished with defined cell-cell contacts. The cytoskeleton was detected as well-spread actin filaments networks. Figure 6c, d, & e show cells differentiated on a PEU/POSS matrix under the same conditions and analyzed by the same methods. Although cells could be detected after TB staining, individual cells could not be distinguished by this method (c) but they could be clearly identified under a fluorescence microscope by the actin staining (d) and by SEM (e). The dramatic change in cell morphology before and after differentiation indicates that the PEU/POSS matrices can provide an environment that supports ESC differentiation and allows for adhesion and spreading of the differentiated cells. It is noted that the cells differentiated on the PEU/POSS matrices were less spread in comparison with cells differentiated on gelatin. This is likely due to the uneven surface of the PEU/POSS matrices and/or different surface chemical properties between gelatin and the PEU/POSS polymer.

3.4. The PEU/POSS matrix provides an excellent interface for cell-matrix interaction

From the results shown in Figure 6c, it appears that differentiated cells were partly embedded into the grooves of the polymer matrix, indicating a close cell-matrix interaction. The matrix structure can be clearly visualized under a fluorescence microscope due to the auto-fluorescence of PEU/POSS polymer, but the polymer can be distinguished from fluorescent-labeled cell components when viewed with different filter sets. To examine the cell-matrix interaction, differentiated cells were double-labeled with FITC-phalloidin for actin-filaments (green) and DAPI for the nuclei (blue), the cell were then examined under high magnification of a conventional fluorescence microscope. For comparison, Figure 7A and B, shows a cell grown on the surface of gelatin-coated coverglass, which has sharply focused actin-filament networks reflecting a well-spread morphology (A) and a crisply defined round nuclei (B). When differentiated cells on the PEU/POSS matrix were examined by the same methods, the nuclei were detected with different intensities and blur images (D and F, indicated by arrows). Similarly, the actin-filaments (C&E, green) were also located at different focal planes relative to the polymer matrix (yellowish auto fluorescence). The cells, as judged by the position of their nuclei and orientation of actin filaments, have intimate contact with the uneven surface of the polymer matrices.

When the samples were examined with a laser scanning confocal microscope, the overall distribution of nuclei and their relationship with the surface of the PEU/POSS matrix can be better demonstrated. Figure 7I & J show a reconstructed 3D image of cells differentiated on a PEU/POSS matrix viewed from two different angles. It is apparent that the cells, judged by the position of nuclei (blue), were tightly embedded on to the grooves of polymer matrix (red background). These results indicated that the surface of the PEU/POSS matrix can provided an interface that allows for cell adhesion and spreading.

4. Discussion

We have previously reported that incorporation of POSS into PEU as a building block affects the mechanical properties, thermostability, and degradability of the polymer (Nanda et al. 2006; Wang et al. 2009). An attractive new feature in the context of tissue engineering is that the PEU/POSS hybrid polymer can form porous matrices. When used for cell culture, it is this porous nature of the matrix that allows cells for better access to growth factors/nutrients and communication through secreted signaling molecules among cells at different locations. In this report, we characterized PEU/POSS thin matrix and investigated the feasibility for their use in ESC-based tissue engineering.

The porosity is mainly attributed to the grooves and pores on the PEU/POSS matrix. Although these structures are randomly distributed, the overall matrix appears rather uniform. While the sizes of most pores are not large enough for cell invasion, together with the grooves that are mostly interconnected, these structures can allow for effective materials exchange. The microscopic analysis gives a direct view of surface topology and the porosity of the thin matrix, but we recognize the fact that this method does not allow for an accurate measurement of the matrix permeability and the degree of pore interconnectivity. These properties are obviously important in cell culture since they can significantly affect cell behavior. While a more rigorous characterization of the matrix will be needed in future studies of the relationship between cell behavior and matrix properties, the current study is focused on investigating the compatibility of the PEU/POSS matrix with ESC culture, which is an important prerequisite for its potential application in ESC-based tissue engineering.

The mechanical properties and the architectures of synthetic biomaterials can be tailored by manipulating their chemical compositions, however, the signals transduced by biologic functional groups of the natural ECM is often difficult to reproduce. The lack of functional

groups is one of the shortfalls of synthetic matrices. Therefore, chemical modification is often needed to improve cell adhesion (Hwang et al. 2008; Yang et al. 2005). However, in doing so the toxicity associated with chemical components involved often cause additional problems. The PEU/POSS matrix exhibits excellent properties in these aspects. Introduction of POSS to PEU polymer does not result in any toxicity to epithelial cells as shown in our previous study (Wang et al. 2009) or to ESCs (this study). Furthermore, the PEU/POSS matrix allows for cell to adhere, proliferate and differentiate without any surface modification. We are not certain at this time what chemical groups on the polymer may provide this capacity, it is speculated that the hydrophilic or charged groups could be involved. Alternatively, some serum proteins contained in the culture medium, such as fibrinogen which is known to promote cell adhesion (Brodbeck et al. 2003), may be adsorbed to the surface of PEU/POSS matrix, which in turn promotes cell adhesion. Judging from the cell number and the expression level of pluripotency makers, it is clear that the PEU/POSS matrix can support ESC proliferation and self-renewal to a similar level provided by gelatin. However, some differences in colony morphology were noted by SEM between cells grown on gelatin and a PEU/POSS matrix. The exact reasons for these observed differences are not clear, but the physical architecture and the surface chemistry, which are obviously different between gelatin and the PEU/POSS matrix, are likely responsible.

ESCs cultured on the PEU/POSS matrix underwent rapid differentiation when cultured in the absence of LIF. Our results demonstrate that the PEU/POSS matrix allows for an intimate cell-cell and cell-matrix interaction. Although grown on an uneven matrix surface, cells showed close contact with neighbor cells and formed a continuous monolayer, indicating that the cells were able to remodel their morphology to form cell-cell adhesion junctions between cells. The location of nuclei and the actin-filaments at the different focal planes relative to the matrix suggest that the cells were able to make close interaction with polymer surface at different locations. Together, these results suggest that the surface architecture of the PEU/POSS matrix can provide a conductive environment for cell-cell/matrix interaction, which is essential for tissue formation. An important unanswered question but we would like to address in the future study is whether the PEU/POSS matrix is able to preferably promote differentiation of certain cell lineages.

In summary, our results demonstrate that the PEU/POSS polymer has properties suitable for fabrication of growth matrices for ESC propagation and differentiation. In addition to the thin matrix described in this study, it is possible to fabricate PEU/POSS polymer into 3D scaffolds with desired porosity, mechanical strength, and biodegradability via precisely synthesis methods (Nanda et al. 2006; Wang et al. 2009). We envision that PEU/POSS polymer may have broad applications in ESC-based soft tissue engineering. However, several properties make them particularly attractive for engineering vascular grafts due to their anti-thromobogenic effect as previously reported (Kannan *et al.*, 2006a). The excellent compatibility of PEU/POSS polymer matrices with ESCs and their derived cells provides a foundation to launch further investigation in that direction.

Acknowledgments

This work was supported by a grant from the National Institutions of Health (HL082731 to Y.-L.G) and a grant from the Division of Chemical, Bioengineering, Environmental, and Transport Systems of the National Science Foundation (CBET 0752150 to J.U.O). We thank Hybrid Plastics (Hattiesburg, Mississippi) for donation of the POSS chemicals and for their technical assistance. We also thank Baobin Kang for microscopy analysis and Mississippi Functional Genomics Network for the use of the facility.

References

Allen M, Svensson L, Roach M, Hambor J, et al. Deficiency of the stress kinase p38{alpha} results in embryonic lethality: characterization of the kinase dependence of stress responses of enzyme-deficient embryonic stem cells. J Exp Med. 2000; 191:859–870. [PubMed: 10704466]

Brodbeck WG, Colton E, Anderson JM. Effects of adsorbed heat labile serum proteins and fibrinogen on adhesion and apoptosis of monocytes/macrophages on biomaterials. J Mat Sci. 2003; 14:671–675.

Burdick JA, Vunjak-Novakovic G. Review: Engineered microenvironments for controlled stem cell differentiation. Tissue Eng Part A. 2000; 14:1–14.

Chai C, Leong KW. Biomaterials approach to expand and direct differentiation of stem cells. Mol Ther. 2007; 15:467–480. [PubMed: 17264853]

Chakraborty S, Kang B, Huang F, Guo YL. Mouse embryonic stem cells lacking p38[alpha] and p38[delta] can differentiate to endothelial cells, smooth muscle cells, and epithelial cells. Differentiation. 2009; 78:143–150. [PubMed: 19539422]

Dawson E, Mapili G, Erickson K, et al. Biomaterials for stem cell differentiation. Adv Drug Deliv Rev. 2008; 60:215–228. [PubMed: 17997187]

Elisseeff J, Ferran A, Hwang S, et al. The role of biomaterials in stem cell differentiation: applications in the musculoskeletal system. Stem Cells Dev. 2006; 15:295–303. [PubMed: 16846368]

Gerecht S, Burdick JA, Ferreira LS, Vunjak-Novakovic G, et al. Hyaluronic acid hydrogel for controlled self-renewal and differentiation of human embryonic stem cells. PNAS. 2007; 104:11298–11303. [PubMed: 17581871]

Guo YL, Yang B. Altered cell adhesion and cell viability in a p38alpha mitogen-activated protein kinase-deficient mouse embryonic stem cell line. Stem Cells Dev. 2006; 15:655–664. [PubMed: 17105401]

Hwang NS, Kim MS, Sampattavanich S, et al. effects of three-dimensional culture and growth factors on the chondrogenic differentiation of murine embryonic stem cells. Stem Cells. 2006; 24:284–291. [PubMed: 16109760]

Hwang NS, Varghese S, Elisseeff J. Controlled differentiation of stem cells. Adv Drug Deliv Rev. 2008; 60:199–214. [PubMed: 18006108]

Kannan RY, Salacinski HJ, DeGroot J, et al. The Antithrombogenic potential of a polyhedral oligomeric silsesquioxane (POSS) nanocomposite. Biomacromolecules. 2006a; 7:215–223. [PubMed: 16398518]

Kannan RY, Salacinski HJ, Sales K, et al. The endothelialization of polyhedral oligomeric silsesquioxane nanocomposites: an in vitro study. Cell Biochem Biophys. 2006b; 45:1–8.

Kannan RY, Salacinski HJ, Edirisinghe MJ, et al. Polyhedral oligomeric silsequioxane-polyurethane nanocomposite microvessels for an artificial capillary bed. Biomaterials. 2006c; 27:4618–4626. [PubMed: 16707157]

Kannan RY, Salacinski HJ, Sales K, et al. The roles of tissue engineering and vascularisation in the development of micro-vascular networks: a review. Biomaterials. 2005; 26:1857–1875. [PubMed: 15576160]

Korley LTJ, Pate BD, Thomas EL, et al. Effect of the degree of soft and hard segment ordering on the morphology and mechanical behavior of semicrystalline segmented polyurethanes. Polymer. 2006; 47:3073–3082.

Lamba, N.; Woodhouse, K.; Cooper, S.; Lelah, M. Polyurethanes in biomedical applications. Boca Raton: CRC press; 1997.

Langer R, Vacanti J. Tissue engineering. Science. 1993; 260:920–926. [PubMed: 8493529]

Nanda AK, Wicks DA, Madbouly SA, et al. Nanostructured polyurethane/POSS hybrid aqueous dispersions prepared by homogeneous solution polymerization. Macromolecules. 2006; 39:7037–7043.

Nelson CM, Bissell MJ. Of Extracellular matrix, scaffolds, and signaling: tissue architecture regulates development, homeostasis, and cancer. Annu Rev Cell Dev Biol. 2006; 22:287–390. [PubMed: 16824016]

Niwa H, Burdon T, Chambers I, et al. Self-renewal of pluripotent embryonic stem cells is mediated via activation of STAT3. Genes Dev. 1998; 12:2048–2060. [PubMed: 9649508]

Nur EK, Ahmed I, Kamal J, et al. Three-Dimensional nanofibrillar surfaces promote self-renewal in mouse embryonic stem cells. Stem Cells. 2006; 24:426–433. [PubMed: 16150921]

O'Connor MD, Kardel MD, Iosfina I, et al. Alkaline phosphatase-positive colony formation is a sensitive, specific, and quantitative indicator of undifferentiated human embryonic stem cells. Stem Cells. 2008; 26:1109–1116. [PubMed: 18276800]

Ouyang A, Ng R, Yang ST. Long-term culturing of undifferentiated embryonic stem cells in conditioned media and three-dimensional fibrous matrices without extracellular matrix coating. Stem Cells. 2007; 25:447–454. [PubMed: 17023515]

Pfaffl MW. A new mathematical model for relative quantification in real-time RT-PCR. Nucl Acids Res. 2001; 29:e45. [PubMed: 11328886]

Raghunath J, Salacinski HJ, Sales KM, et al. Advancing cartilage tissue engineering: the application of stem cell technology. Curr Opin Biotechnol. 2005; 16:503–509. [PubMed: 16153817]

Saha K, Pollock JF, Schaffer DV, et al. Designing synthetic materials to control stem cell phenotype. Curr Opin Chem Biol. 2007; 11:381–387. [PubMed: 17669680]

Wang W, Guo YL, Otaigbe JU. The synthesis, characterization and biocompatibility of poly(ester urethane)/polyhedral oligomeric silesquioxane nanocomposites. Polymer. 2009; 50:5749–5757.

Wang W, Guo Y, Otaigbe JU. Synthesis and characterization of novel biodegradable and biocompatible poly(ester-urethane) thin films prepared by homogeneous solution polymerization. Polymer. 2008; 49:4393–4398.

Wang Y, Kim HJ, Vunjak-Novakovic G, et al. Stem cell-based tissue engineering with silk biomaterials. Biomaterials. 2006; 27:6064–6082. [PubMed: 16890988]

Wobus AM, Boheler KR. Embryonic stem cells: prospects for developmental biology and cell therapy. Physiol Rev. 2005; 85:635–678. [PubMed: 15788707]

Yang F, Williams CG, Wang Da, et al. The effect of incorporating RGD adhesive peptide in polyethylene glycol diacrylate hydrogel on osteogenesis of bone marrow stromal cells. Biomaterials. 2005; 26:5991–5998. [PubMed: 15878198]

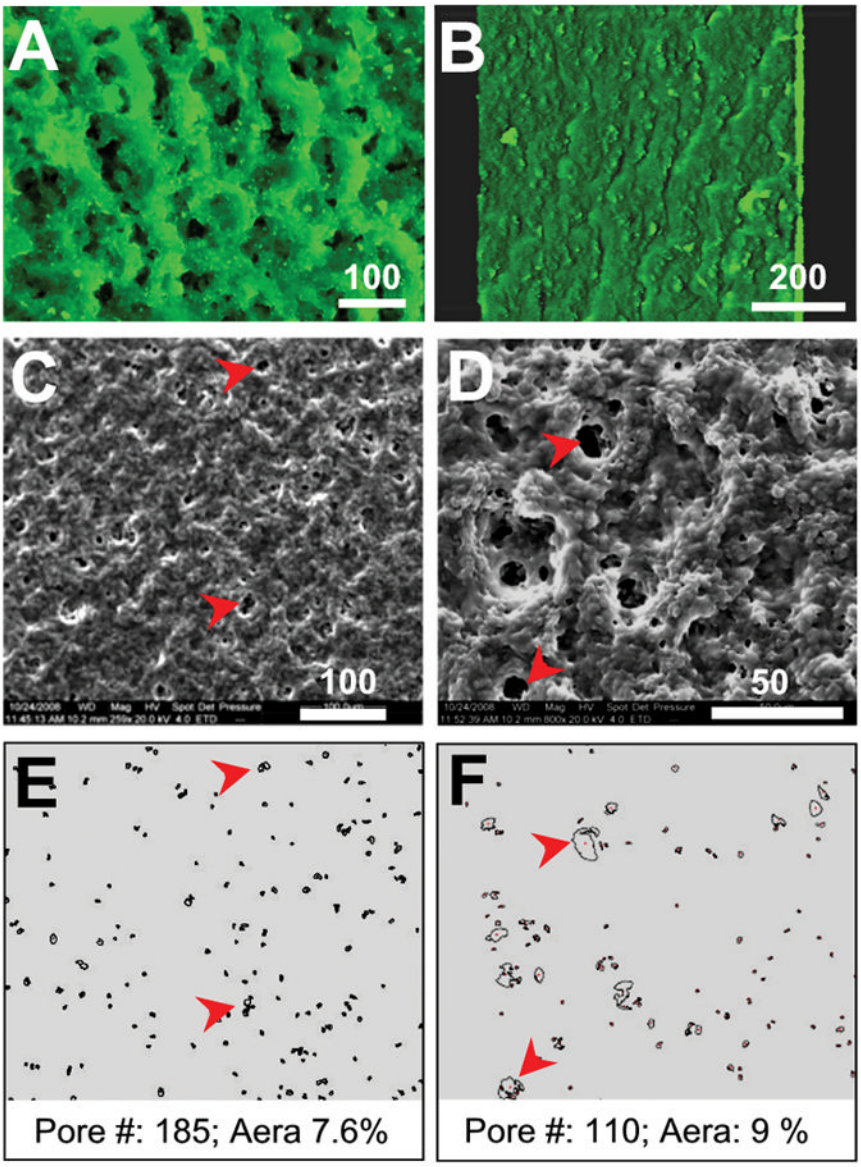

Figure 1. Microscopic analysis of architecture and surface topology of PEU/POSS thin film matrices

A, The porous matrix visualized under a Nikon fluorescence microscope (Eclipse 80i, Plan Fluor 10X/0.75 DIC M/N2 lens with filters set for FITC). **B,** surface topology examined with a LSM510 laser-scanning confocal microscope (Zeiss) under the configuration of excitation at 488 nm and emission at 505 nm. This 3D projection of the surface structure was reconstructed from a Z-stack consisting 30 sections (1.5 μm/section). **C & D,** surface structure analyzed with a SEM (FEI Quanta 200) at two different magnifications (two pores in each image were indicated by arrow, bar unit =μm). **E & F,** Images of pores and their distribution traced from SEM images C and D, respectively. The number of pores and area coverage were automatically calculated using Image J software. 1 μm^2 was set as the minimum pore size for selection.

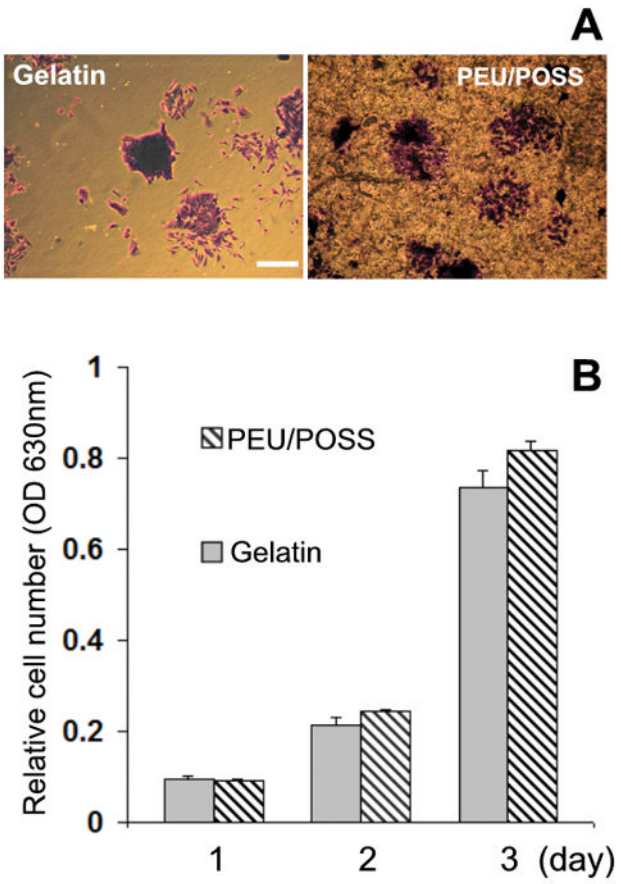

Figure 2. ESC proliferation on gelatin and on the PEU/POSS matrix

A, 5000 ESCs were seeded on gelatin-coated coverglasses or on a PEU/POSS matrix and cultured in a 24 well plate. The cells were fixed and stained with toluidine blue (TB). Cell density and colonies of ESCs were examined under a phase contrast microscope (photos, bar = 200 μm). **B,** The total number of cells was indirectly represented by the absorbance at 630 nm of TB extracted from stained cells that were cultured at the different times as indicated. The Results are means ± SD of duplicate assays. Differences are not significant between two groups at all times tested (Statistical analysis was performed using a two-tailed unpaired Student *t* test. Differences are considered statistically significant when $p<0.05$).

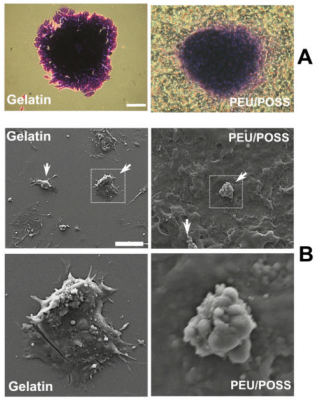

Figure 3. Cell and colony morphology of ESCs grown on gelatin and on the PEU/POSS matrix

A, Cell and colony morphology of ESCs stained with toluidine blue (TB) and examined under a phase contrast microscope (bar = 50 μm). **B.** Cell and colony morphology of ESCs examined with a SEM (upper panels bar = 200 μm). Arrows indicate representative colonies of similar sizes. The images in the lower panels are the enlarged box areas of upper panels as indicted.

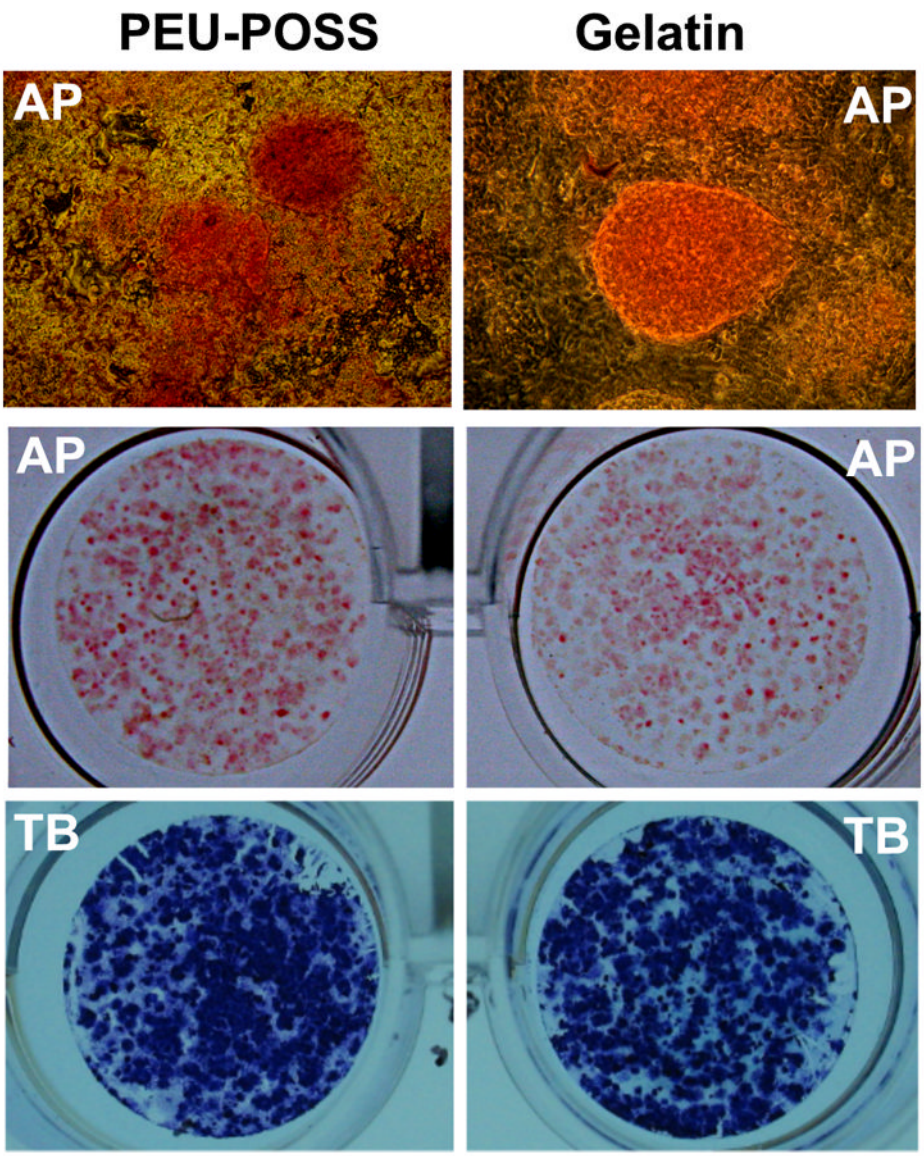

Figure 4. Alkaline phosphatase activity analysis in ESC colonies grown on gelatin and the PEU/POSS matrix

6-day colonies were stained with an alkaline phosphatase (AP) Kit. AP positive colonies were identified by their red color. Top panels, images photographed under a phase contrast microscope (10 × objective lens); middle panels, photographs of AP positive colonies in whole culture dishes; bottom panels; photographs of TB stained all ESC populations.

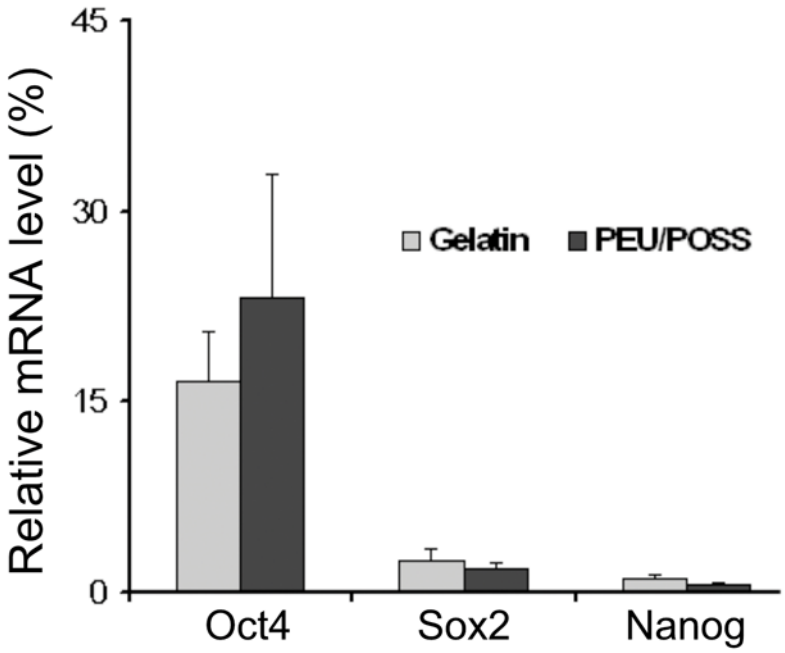

Figure 5. Expression of pluripotency markers in ESCs grown on gelatin and the PEU/POSS matrix

Total RNA was extracted from ESCs grown on gelatin or on a PEU/POSS matrix. The mRNA level of each gene was determined by qRT-PCR in duplicates and was normalized to β-actin mRNA. The expression level of β-actin was set as 100 %. Results are means ± SEM of three independent experiments. Differences are not significant between two groups for all genes tested (Statistical analysis was performed using a two-tailed unpaired Student *t* test. Differences are considered statistically significant when $p<0.05$).

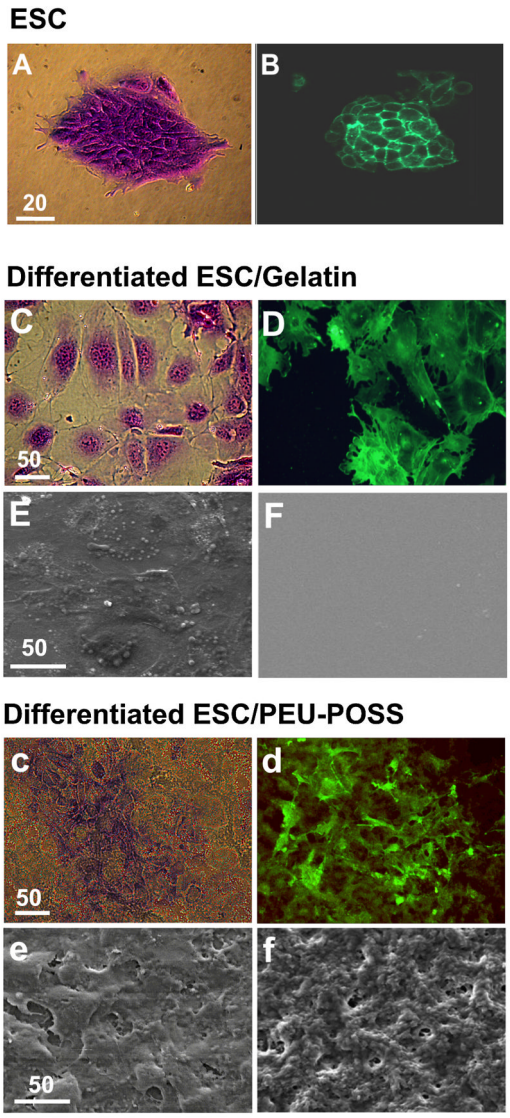

Figure 6. Morphology of undifferentiated ESCs and differentiated cells grown on gelatin and on the PEU/POSS matrix

A and B, a colony of undifferentiated ESCs photographed under a phase contrast microscope (A, cells stained with TB) or under a fluorescence microscope (B, cells labeled with FITC-phalloidin); C, D, and E, ESCs differentiated on gelatin; c, d, and e, ESCs differentiated on a PEU/POSS matrix. C & c are cells stained with TB; D & d are cells labeled with FITC-phalloidin. E & e are cells analyzed with SEM; and F & f are SEM images of the surface of a coverglass coated with gelatin and the surface of a PEU/POSS matrix, respectively, before cell seeding (scale bar unit is μm).

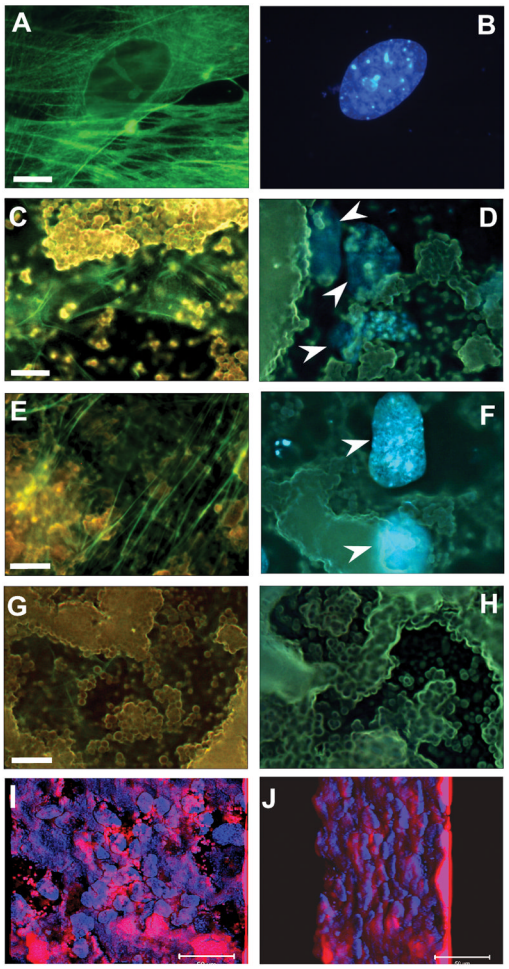

Figure 7. Microscopic analysis of cell-matrix interaction

A and B, ESCs differentiated on a gelatin-coated coverglass analyzed under an Olympus fluorescence microscope (A, actin filaments labeled with FITC-phalloidin; B, the nucleus labeled with DAPI); C-J, ESCs differentiated on the PEU/POSS matrix analyzed under an Olympus fluorescence microscope (C & E, two representative images of actin filaments); D & F, two representative images of the nuclei, indicated by arrows; G & H, polymers detected by their auto-fluorescence under a FITC filter set and DAPI filter set, respectively); I & J, ESCs differentiated on a PEU/POSS matrix analyzed with a LSM510 laser-scanning confocal microscope under the configurations of excitation 405 nm/emission 420–480 nm to detect nuclei (blue) and excitation 543 nm/emission 560 nm to detect auto-fluorescence of the polymer (red). The image is a 3D projection reconstructed from a Z-stack consisting 62 sections (1.5 μm/section) and viewed from two different angles. Nuclei labeled with DAPI were shown blue and the polymer matrix is shown as red background (scale bars, A-H = 10 μm, I & J = 50 μm).